Journal of General Virology (2012), **93**, 1918–1923 **DOI** 10.1099/vir.0.043190-0

Short Communication

Organ tropism of murine coronavirus does not correlate with the expression levels of the membrane-anchored or secreted isoforms of the carcinoembryonic antigen-related cell adhesion molecule 1 receptor

Olga Slobodskaya, Eric J. Snijder and Willy J. M. Spaan

Molecular Virology Laboratory, Department of Medical Microbiology, Center of Infectious Diseases, Leiden University Medical Center, The Netherlands

Correspondence
Olga Slobodskaya
o.slobodskaya@gmail.com
Eric J. Snijder
e.j.snijder@lumc.nl

Received 25 March 2012
Accepted 31 May 2012

Carcinoembryonic antigen-related cell adhesion molecule 1 (CEACAM1) is the sole known receptor of murine hepatitis virus (MHV) A59, but the available, often qualitative, data about CEACAM1 expression does not explain MHV organ tropism. *Ceacam1* transcripts undergo alternative splicing resulting in multiple isoforms, including secreted CEACAM1 isoforms that can neutralize the virus. We determined the quantities of *Ceacam1* transcripts encoding membrane-bound and secreted isoforms in mouse organs and a set of cell lines. *In vivo*, the lowest receptor mRNA levels were found in brain and muscle and these were similar to those in easily infectable cultured cells. While the quantities of the receptor transcripts varied between mouse organs, their abundance did not correlate with susceptibility to MHV infection. The proportion of transcripts encoding secreted isoforms also could not explain the selection of sites for virus replication, as it was constant in all organs. Our data suggest that neither of the two CEACAM1 isoforms defines MHV organ tropism.

Receptors are essential determinants of host susceptibility to virus infections. In some cases, the pattern of receptor expression is the major factor defining organ, tissue and cell tropism of a virus (Maddon *et al.*, 1986). In other cases, additional factors modulate viral replication at sites with sufficient receptor amounts. Local innate immunity can restrict virus replication in potentially susceptible organs (Ida-Hosonuma *et al.*, 2005). Tissue-specific alternative splicing of receptor transcripts may control infection spread within a body (Kohaar *et al.*, 2010).

Murine hepatitis virus strain A59 (MHV-A59), one of the prototypic coronaviruses, uses carcinoembryonic antigen-related cell adhesion molecule 1 (CEACAM1) as a receptor (Dveksler *et al.*, 1991; Hemmila *et al.*, 2004), although the quantities of CEACAM1 do not explain MHV-A59 organ tropism in mice (Bender *et al.*, 2010; Godfraind *et al.*, 1995). MHV was found in the highly expressing small intestine and liver, but also in organs with low CEACAM1 amounts, such as lung and brain (Barthold & Smith, 1984; Lavi *et al.*, 1986; Raaben *et al.*, 2009). Remarkably, the virus fails to infect kidneys, despite their high CEACAM1 expression level (Barthold & Smith, 1984). In addition to mediating virus entry, CEACAM1 promotes cell-to-cell fusion (Vennema *et al.*, 1990) and may be directly responsible for the cytotoxicity of MHV infection (Rao & Gallagher, 1998).

CEACAM1 belongs to a multimember family of membrane-anchored and soluble CEA proteins containing immunoglobulin (Ig)-like domains (Beauchemin *et al.*, 1999). CEACAM1 participates in homophilic and heterophilic interactions and is involved in the regulation of cell growth and signalling (Chen *et al.*, 2009; Öbrink, 1997). The development of some tumours correlates with either up- or downregulation of CEACAM1 expression (Hammarström, 1999; Öbrink, 2008), although the mechanism of its action in promoting or suppressing tumour growth remains unclear. The mouse *Ceacam1* gene contains nine exons (Fig. 1) and alternative splicing of *Ceacam1* transcripts plays an important role in the regulation of its function (Chen *et al.*, 2009). Some findings suggest that it is not the general CEACAM1 expression level that is linked to oncogenesis, but rather the ratio of the protein's isoforms (Gaur *et al.*, 2008; Singer *et al.*, 2000), especially CEACAM1-4 containing four Ig-like domains (N, A1, B and A2) versus CEACAM1-2 having two such domains (N and A2), and CEACAM1-L versus CEACAM1-S, which have long and short cytoplasmic tails (CT), respectively. Interestingly, the relative abundance of CEACAM1 isoforms is a dynamic parameter that correlates with cell density (Singer *et al.*, 2000). Secreted isoforms lacking the transmembrane domain (TM) were identified in humans and rodents (Budt *et al.*, 2002; Kuroki *et al.*,

1991; Terahara *et al.*, 2009), but remain poorly characterized despite the use of soluble CEACAM1 detection in body fluids in cancer diagnostics (Hundt *et al.*, 2007; Simeone *et al.*, 2007). Notwithstanding the variety and multifunctionality of CEACAM1 isoforms, the physiological role of the protein turned out to be sufficiently redundant for knockout Ceacam1$^{-/-}$ mice to be viable and fertile (Hemmila *et al.*, 2004).

Different isoforms of mouse CEACAM1 were shown to be competent MHV receptors (Dveksler *et al.*, 1993). The prevalence of CEACAM1-4 versus CEACAM1-2, as well as CEACAM1-L versus CEACAM1-S, does not account for MHV-A59 tropism within the mouse central nervous system (Bender *et al.*, 2010). Recombinant soluble CEACAM1 lacking the TM domain neutralized MHV *in vitro* (Schickli *et al.*, 1997; Terahara *et al.*, 2009), indicating its capability to influence MHV infection *in vivo*.

We were interested to find out whether a threshold amount of *Ceacam1* expression is required to allow MHV infection and whether the expression pattern of secreted isoforms of the receptor contributes to MHV organ tropism.

In order to obtain a reference set for *Ceacam1* expression measurements in mice and to establish the quantitative relationship between mRNA and protein levels, we determined the amounts of membrane-anchored CEACAM1 and corresponding *Ceacam1* transcripts in eight cell types. These belonged to six distinct cell lines derived from different mouse strains: four were fibroblast-like, NIH 3T3 (NIH Swiss mouse), 17Cl-1 (BALB/c), Sac(−) (STU) and L929 (C3H/An), one was myoblast-like C2C12 (C3H), and the last one was the astrocytoma-derived DBT (CDF1) cell line. Two of the cell lines, 17Cl-1 and L929, were each represented by two lineages from different sources and with different passage history. Descendants of the 17Cl-1 line originated from Dr P. Rottier's laboratory (17Cl-1U; Utrecht University, Utrecht, the Netherlands) or were obtained from Dr S. Siddell (17Cl-1S; University of Bristol, Bristol, UK). The latter had been grown from a single cell and selected for high MHV production (S. Sawicki, personal communication; Sawicki *et al.*, 1995). The L929 cell line was represented by a culture passaged less than six times after the delivery from the American type culture collection (L929) and a L929-descendant (L) with a long passage history originating from Dr P. Rottier's laboratory. All cell lines were susceptible to productive MHV-A59 infection, which was non-cytopathogenic in C2C12 and NIH 3T3 cells and cytopathogenic in the others (Slobodskaya *et al.*, 2008).

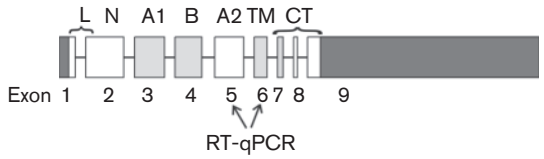

Fig. 1. *Ceacam1* gene structure. The nine *Ceacam1* exons are shown as rectangles (up to scale), while introns (not to scale) are depicted by lines. Light grey shaded (boxes) exons 3, 4, 6 and 7 may be spliced out. Dark grey areas represent 5′- and 3′-non-coding regions. The segments encoding leader L, four Ig-like domains N, A1, B and A2, TM and CT are indicated above the transcript. RT-qPCR assays specific for the exons 5 and 6 were used to quantify all *Ceacam1* transcripts and transcripts encoding all membrane-bound isoforms, respectively.

Cells harvested from one dish were divided into two parts, one used for RNA extraction and transcript analysis and the other for the flow-cytometrical analysis of the expression level of membrane-anchored CEACAM1. Compared to earlier results (Slobodskaya *et al.*, 2008), the use of a second antibody conjugated to allophycocyanin instead of fluorescein-isothiocyanate markedly improved the signal to noise ratio during flow cytometry. With the improved resolution between CEACAM1-positive and autofluorescent control cells, it became obvious that in all but one of the cell lines the majority of the cells (60–100 %) were truly CEACAM1-positive (Fig. 2a). It remained unresolved whether the majority of C2C12 cells were weakly CEACAM1-positive or truly negative. The heterogeneity of CEACAM1 amounts on the surface of individual cells in a population (illustrated by the peak width in Fig. 2a) differed between cell types. The same was true for the total amount of surface-expressed protein, which differed up to 100-fold between cell populations (Fig. 2b). Remarkably, cells having the same origin, but a different history, 17Cl-1S and 17Cl-1U, displayed a 10-fold difference in the amounts of CEACAM1.

We determined relative amounts and ratio of transcripts encoding membrane-anchored and secreted CEACAM1 isoforms. The quantity of the first transcript was also compared to the amount of the corresponding protein. Transcripts specifying membrane-anchored CEACAM1 isoforms all contain the 121 nt long exon 6, which encodes the TM (Fig. 1). The amount of these transcripts (mRNA TM+) was determined with the use of the exon 6-specific primers 5′-CATTGCTGGCATCGTGATT-3′ and 5′-CGCCAGACTTCCTGGAATAG-3′. We also measured the total amount of *Ceacam1* transcripts (mRNA all) by targeting exon 5 (primers 5′-CCAACACCACAGTCAAAGAACTA-3′ and 5′-GTGAGCTGAAGACTCTGGCTATT-3′), which is present in all *Ceacam1* mRNAs (Fig. 1). The difference between amounts of mRNA all and mRNA TM+ gave the quantity of *Ceacam1* transcripts specifying secreted isoforms (mRNA TM−). RT-qPCR was performed as described elsewhere (Versteeg *et al.*, 2006) with an additional DNase I treatment of the RNA prior to reverse transcription. The relative amounts of *Ceacam1* mRNA were determined using standard curves obtained with a plasmid containing a cDNA copy of a nine-exon-containing CEACAM1 variant. Transcript amounts were normalized to the amounts of 18S rRNA (primers 5′-CCCAGTAAGTGCGGGTCATA-3′ and 5′-GATCCGAGGGCCTCACTAAA-3′) determined in the same samples.

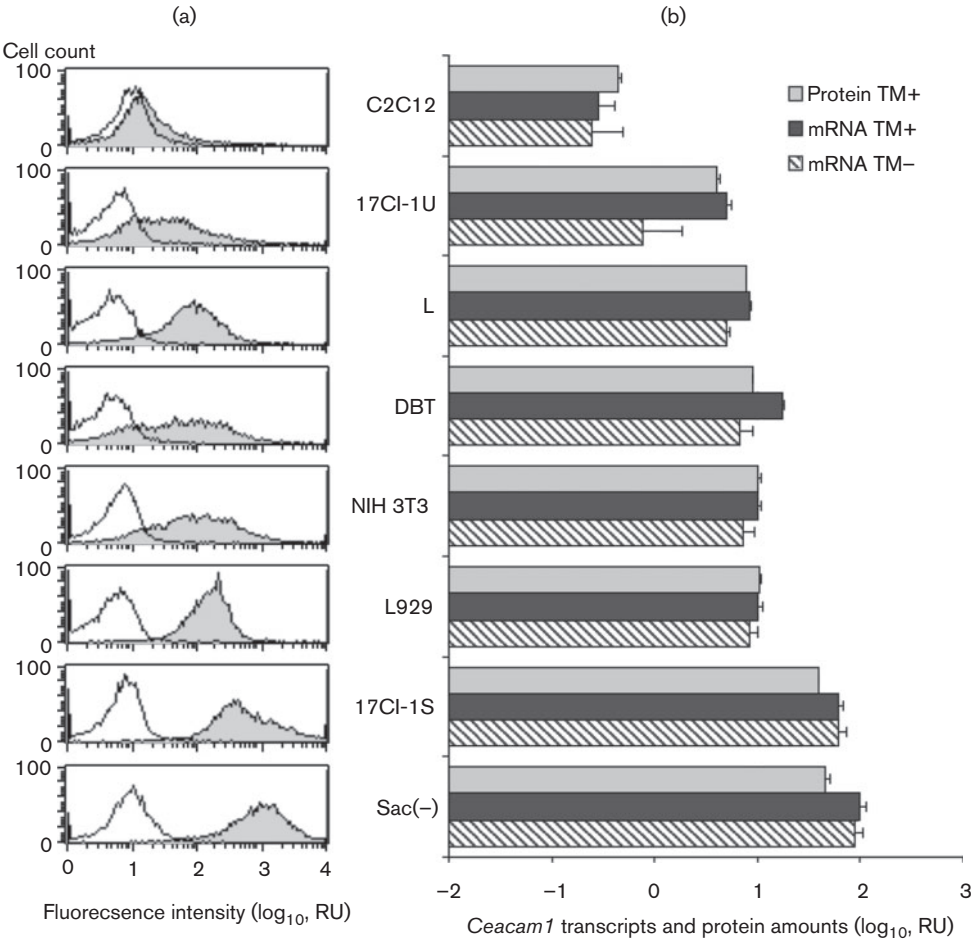

Fig. 2. Cell surface-bound CEACAM1 protein and *Ceacam1* transcripts in mouse cell lines. (a) The amount of protein on the cell surface was determined by labelling with anti-CEACAM1 mAb CC1 and using flow cytometry. Shaded and non-shaded peaks show CEACAM1-labelled and control cells, respectively, in representative histograms. (b) The relative amount of membrane-anchored CEACAM1 (protein TM+) in the cell populations was calculated by multiplying the proportion of CEACAM1-positive cells by the mean fluorescence intensity of these cells, both determined by flow cytometry. The relative amount of *Ceacam1* transcripts encoding membrane-anchored (mRNA TM+) or secreted protein (mRNA TM–) was determined with the use of RT-qPCR. The scale was chosen so that the quantities of both CEACAM1 protein and exon 6-containing *Ceacam1* transcript in NIH 3T3 cells equalled 10 RU. Error bars represent ranges (flow cytometry, $n=2$) or SD (RT-qPCR, $n=3$). RU, Relative units.

The quantity of the transcripts containing the TM domain-encoding exon 6 (mRNA TM+) showed a direct correlation with the amount of membrane protein (Protein TM+; coefficient 0.97) (Fig. 2b). The ratio of the concentrations of a protein and its corresponding mRNA depends on the rates of synthesis and decay of both molecules (Schwanhäusser *et al.*, 2011). We found that for membrane-anchored CEACAM1 this ratio was similar in cells of different origin and genetic backgrounds, and the quantity of the exon 6-containing mRNA reflected the amount of the protein.

The molar ratio of *Ceacam1* transcripts encoding TM+ and TM− isoforms varied between 1 and 6.5 and did not correlate with the general level of *Ceacam1* gene expression or cell density. This ratio was found to be 1–1.2 in low- (C2C12) and high-expressing cells [L929, 17Cl-1S and Sac(−)], while in four other cultures the mRNA TM+ was more abundant, with the ratios being 1.4 (NIH 3T3), 1.7 (L), 2.6 (DBT) and 6.5 (17Cl-1U). Due to cell size differences, comparison of their density was not informative for cells of different origin. However, the 17Cl-1 sublines, 17Cl-1U and 17Cl-1S, with similar cell size and density at the time of harvest ($1.1–1.4 \times 10^4$ cells cm^{-2}), had the most dissimilar ratio of *Ceacam1* transcripts (6.5 and 1.0, respectively), suggesting that factors other than cell density affect generation of these splice variants.

We examined *Ceacam1* gene expression in brain, liver, small intestine, spleen, kidney, lung and muscle of

3-week-old MHV-susceptible C57Bl/6 mice (Fig. 3). While organs consist of different tissues and cell types, which might differ in regard to *Ceacam1* expression, the average receptor amounts determined here reflect the number of potential entry sites for the virus within the organs. Brain and muscle had the smallest quantities of total *Ceacam1* mRNA (mRNA all) [32 and 68 relative units (RU), respectively]. Intermediate amounts (210–890 RU) were found in spleen, lung, kidney and liver. Small intestine was characterized by a remarkably high expression level of the *Ceacam1* gene (23 680 RU). Notably, the proportion of transcripts encoding soluble protein was rather constant in all mouse organs, with a mean of 47 % (42–53 %). In general, there was a good agreement between our quantitative data and previously published studies of CEACAM1 protein and mRNA detection (Fig. 3).

The ease of MHV infection in cultured cells suggested that CEACAM1 amounts *in vitro* may surpass the amounts in mouse tissues. Contrary to this expectation, the two ranges of CEACAM1 quantities, *in vitro* (Fig. 2b) and *in vivo* (Fig. 3), hardly overlapped and the majority of the transformed cell lines had lower levels of *Ceacam1* transcripts than normal mouse tissues. Only Sac(−) (185 RU) and 17Cl-1S (122 RU) cells with the highest *Ceacam1* mRNA levels reached those in the mouse organs.

Cell surface-bound receptors may contribute to the efficiency of the initial rounds of infection, to the rate of viral spread within a tissue or organ and to the cytopathogenicity of infection. Secreted isoforms may have an inhibitory role in infection by neutralizing the virus or preventing cell-to-cell fusion. Comparison of our *Ceacam1* data with the evidence of MHV replication published earlier (Fig. 3) yielded the following conclusions.

In vitro a broad range of cell surface receptor levels allowed virus infection. Comparison of the *in vivo* and *in vitro* data suggested that cells in all tested organs express sufficient amounts of membrane-bound receptor to make them susceptible to infection. For instance, cells in mouse brain, an organ with the lowest level of *Ceacam1* transcripts, express on average twice as much receptor as the readily infectable L929 cell line.

The levels of the transcript for membrane-bound CEACAM1 did not correlate with the presence of virus in mouse organs during infection. For instance, muscle and brain have similar amounts of *Ceacam1* transcripts, but muscle shows no signs of virus replication while the brain is permissive to virus infection. The same holds true for kidneys and lung (Fig. 3). Brain, spleen and small intestine, having the lowest, intermediate and highest *Ceacam1* gene expression, respectively, were all characterized by a low level of virus replication. On the other hand, virus was most consistently found in the liver and lung, both organs with intermediate amounts of *Ceacam1* transcripts.

The levels of the transcript for secreted CEACAM1 isoforms or the ratio of amounts of transcripts encoding secreted and membrane-anchored proteins also did not match MHV organ tropism. In addition, secreted receptor also could not explain the resistance of C2C12 and NIH

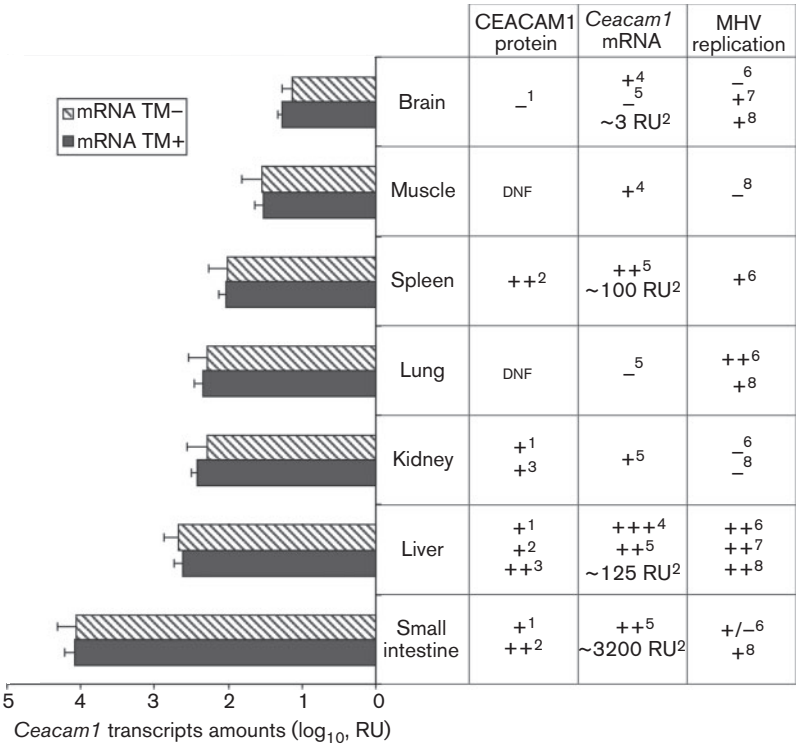

	CEACAM1 protein	*Ceacam1* mRNA	MHV replication
Brain	−[1]	+[4] −[5] ~3 RU[2]	−[6] +[7] +[8]
Muscle	DNF	+[4]	−[8]
Spleen	++[2]	++[5] ~100 RU[2]	+[6]
Lung	DNF	−[5]	++[6] +[8]
Kidney	+[1] +[3]	+[5]	−[6] −[8]
Liver	+[1] +[2] ++[3]	+++[4] ++[5] ~125 RU[2]	++[6] ++[7] ++[8]
Small intestine	+[1] ++[2]	++[5] ~3200 RU[2]	+/−[6] +[8]

Fig. 3. *Ceacam1* gene expression and MHV infection in mouse organs. The graph on the left shows the relative amounts of *Ceacam1* transcripts encoding membrane-anchored (mRNA TM+) and secreted (mRNA TM−) isoforms in the organs of C57Bl/6 mice determined as described in the legend to Fig. 2. The table on the right summarizes published results obtained with the use of: [1], immunofluorescence microscopy (IFM) of CEACAM1 (Godfraind *et al.*, 1995); [2], [3], CEACAM1 IFM and Western blot analysis (Hirai *et al.*, 2010), (Blau *et al.*, 2001); [4], [5], RT followed by semi-quantitative PCR of *Ceacam1* transcripts (Yokomori & Lai, 1992), (Han *et al.*, 2001); [2], RT-qPCR of *Ceacam1* transcripts (Hirai *et al.*, 2010); [6], IFM of MHV proteins (Barthold & Smith, 1984); [7], pathology and MHV titration (Lavi *et al.*, 1986); [8], live imaging of MHV replication (Raaben *et al.*, 2009). These data were obtained for CD-1, C57BL/6 and BALB/c mice, which have similar susceptibility to MHV infection. DNF, Data not found.

3T3 cells to virus-induced cell damage as both its quantities and ratios fall within the ranges found in cells with cytopathogenic infection.

The extent of receptor exposure and its involvement in interactions with neighbouring cells will influence the actual number of sites available for virus binding. This factor, which is determined by the specific architecture of an organ, together with the other, yet unknown, factors modulating virus entry and the intracellular phase of virus reproduction (Bender *et al.*, 2010; Slobodskaya *et al.*, 2008; Taguchi & Hirai-Yuki, 2012) plus the local innate immunity profiles (Zhao *et al.*, 2011) most probably define the tissue and organ tropism of MHV.

Acknowledgements

We are grateful to Stuart Siddell and Stanley Sawicki for 17Cl-1S cells and to Kathryn Holmes for CC1 mAb. We thank our colleagues Peter Bredenbeek and Tim Dalebout for their help with animal experiments.

References

Barthold, S. W. & Smith, A. L. (1984). Mouse hepatitis virus strain-related patterns of tissue tropism in suckling mice. *Arch Virol* **81**, 103–112.

Beauchemin, N., Draber, P., Dveksler, G., Gold, P., Gray-Owen, S., Grunert, F., Hammarström, S., Holmes, K. V., Karlsson, A. & other authors (1999). Redefined nomenclature for members of the carcinoembryonic antigen family. *Exp Cell Res* **252**, 243–249.

Bender, S. J., Phillips, J. M., Scott, E. P. & Weiss, S. R. (2010). Murine coronavirus receptors are differentially expressed in the central nervous system and play virus strain-dependent roles in neuronal spread. *J Virol* **84**, 11030–11044.

Blau, D. M., Turbide, C., Tremblay, M., Olson, M., Létourneau, S., Michaliszyn, E., Jothy, S., Holmes, K. V. & Beauchemin, N. (2001). Targeted disruption of the Ceacam1 (MHVR) gene leads to reduced susceptibility of mice to mouse hepatitis virus infection. *J Virol* **75**, 8173–8186.

Budt, M., Michely, B., Müller, M. M., Reutter, W. & Lucka, L. (2002). Secreted CEACAM1 splice variants in rat cell lines and in vivo in rat serum. *Biochem Biophys Res Commun* **292**, 749–755.

Chen, Z., Chen, L. & Blumberg, R. S. (2009). Editorial: CEACAM1: fine-tuned for fine-tuning. *J Leukoc Biol* **86**, 195–197.

Dveksler, G. S., Pensiero, M. N., Cardellichio, C. B., Williams, R. K., Jiang, G. S., Holmes, K. V. & Dieffenbach, C. W. (1991). Cloning of the mouse hepatitis virus (MHV) receptor: expression in human and hamster cell lines confers susceptibility to MHV. *J Virol* **65**, 6881–6891.

Dveksler, G. S., Dieffenbach, C. W., Cardellichio, C. B., McCuaig, K., Pensiero, M. N., Jiang, G. S., Beauchemin, N. & Holmes, K. V. (1993). Several members of the mouse carcinoembryonic antigen-related glycoprotein family are functional receptors for the coronavirus mouse hepatitis virus-A59. *J Virol* **67**, 1–8.

Gaur, S., Shively, J. E., Yen, Y. & Gaur, R. K. (2008). Altered splicing of CEACAM1 in breast cancer: identification of regulatory sequences that control splicing of CEACAM1 into long or short cytoplasmic domain isoforms. *Mol Cancer* **7**, 46.

Godfraind, C., Langreth, S. G., Cardellichio, C. B., Knobler, R., Coutelier, J. P., Dubois-Dalcq, M. & Holmes, K. V. (1995). Tissue and cellular distribution of an adhesion molecule in the carcinoembryonic antigen family that serves as a receptor for mouse hepatitis virus. *Lab Invest* **73**, 615–627.

Hammarström, S. (1999). The carcinoembryonic antigen (CEA) family: structures, suggested functions and expression in normal and malignant tissues. *Semin Cancer Biol* **9**, 67–81.

Han, E., Phan, D., Lo, P., Poy, M. N., Behringer, R., Najjar, S. M. & Lin, S. H. (2001). Differences in tissue-specific and embryonic expression of mouse Ceacam1 and Ceacam2 genes. *Biochem J* **355**, 417–423.

Hemmila, E., Turbide, C., Olson, M., Jothy, S., Holmes, K. V. & Beauchemin, N. (2004). Ceacam1a-/- mice are completely resistant to infection by murine coronavirus mouse hepatitis virus A59. *J Virol* **78**, 10156–10165.

Hirai, A., Ohtsuka, N., Ikeda, T., Taniguchi, R., Blau, D., Nakagaki, K., Miura, H. S., Ami, Y., Yamada, Y. K. & other authors (2010). Role of mouse hepatitis virus (MHV) receptor murine CEACAM1 in the resistance of mice to MHV infection: studies of mice with chimeric mCEACAM1a and 1b. *J Virol* **84**, 6654–6666.

Hundt, S., Haug, U. & Brenner, H. (2007). Blood markers for early detection of colorectal cancer: a systematic review. *Cancer Epidemiol Biomarkers Prev* **16**, 1935–1953.

Ida-Hosonuma, M., Iwasaki, T., Yoshikawa, T., Nagata, N., Sato, Y., Sata, T., Yoneyama, M., Fujita, T., Taya, C. & other authors (2005). The alpha/beta interferon response controls tissue tropism and pathogenicity of poliovirus. *J Virol* **79**, 4460–4469.

Kohaar, I., Ploss, A., Korol, E., Mu, K., Schoggins, J. W., O'Brien, T. R., Rice, C. M. & Prokunina-Olsson, L. (2010). Splicing diversity of the human OCLN gene and its biological significance for hepatitis C virus entry. *J Virol* **84**, 6987–6994.

Kuroki, M., Arakawa, F., Matsuo, Y., Oikawa, S., Nakazato, H. & Matsuoka, Y. (1991). Three novel molecular forms of biliary glycoprotein deduced from cDNA clones from a human leukocyte library. *Biochem Biophys Res Commun* **176**, 578–585.

Lavi, E., Gilden, D. H., Highkin, M. K. & Weiss, S. R. (1986). The organ tropism of mouse hepatitis virus A59 in mice is dependent on dose and route of inoculation. *Lab Anim Sci* **36**, 130–135.

Maddon, P. J., Dalgleish, A. G., McDougal, J. S., Clapham, P. R., Weiss, R. A. & Axel, R. (1986). The T4 gene encodes the AIDS virus receptor and is expressed in the immune system and the brain. *Cell* **47**, 333–348.

Öbrink, B. (1997). CEA adhesion molecules: multifunctional proteins with signal-regulatory properties. *Curr Opin Cell Biol* **9**, 616–626.

Öbrink, B. (2008). On the role of CEACAM1 in cancer. *Lung Cancer* **60**, 309–312.

Raaben, M., Prins, H. J., Martens, A. C., Rottier, P. J. & De Haan, C. A. (2009). Non-invasive imaging of mouse hepatitis coronavirus infection reveals determinants of viral replication and spread in vivo. *Cell Microbiol* **11**, 825–841.

Rao, P. V. & Gallagher, T. M. (1998). Intracellular complexes of viral spike and cellular receptor accumulate during cytopathic murine coronavirus infections. *J Virol* **72**, 3278–3288.

Sawicki, S. G., Lu, J. H. & Holmes, K. V. (1995). Persistent infection of cultured cells with mouse hepatitis virus (MHV) results from the epigenetic expression of the MHV receptor. *J Virol* **69**, 5535–5543.

Schickli, J. H., Zelus, B. D., Wentworth, D. E., Sawicki, S. G. & Holmes, K. V. (1997). The murine coronavirus mouse hepatitis virus strain A59 from persistently infected murine cells exhibits an extended host range. *J Virol* **71**, 9499–9507.

Schwanhäusser, B., Busse, D., Li, N., Dittmar, G., Schuchhardt, J., Wolf, J., Chen, W. & Selbach, M. (2011). Global quantification of mammalian gene expression control. *Nature* **473**, 337–342.

Simeone, D. M., Ji, B., Banerjee, M., Arumugam, T., Li, D., Anderson, M. A., Bamberger, A. M., Greenson, J., Brand, R. E. & other authors (2007). CEACAM1, a novel serum biomarker for pancreatic cancer. *Pancreas* **34**, 436–443.

Singer, B. B., Scheffrahn, I. & Öbrink, B. (2000). The tumor growth-inhibiting cell adhesion molecule CEACAM1 (C-CAM) is differently expressed in proliferating and quiescent epithelial cells and regulates cell proliferation. *Cancer Res* **60**, 1236–1244.

Slobodskaya, O., Laarman, A. & Spaan, W. J. (2008). Intracellular restriction of a productive noncytopathic coronavirus infection. *J Virol* **82**, 451–460.

Taguchi, F. & Hirai-Yuki, A. (2012). Mouse hepatitis virus receptor as a determinant of the mouse susceptibility to MHV infection. *Front Microbiol* **3**, 68.

Terahara, K., Yoshida, M., Taguchi, F., Igarashi, O., Nochi, T., Gotoh, Y., Yamamoto, T., Tsunetsugu-Yokota, Y., Beauchemin, N. & Kiyono, H. (2009). Expression of newly identified secretory CEACAM1(a) isoforms in the intestinal epithelium. *Biochem Biophys Res Commun* **383**, 340–346.

Vennema, H., Heijnen, L., Zijderveld, A., Horzinek, M. C. & Spaan, W. J. (1990). Intracellular transport of recombinant coronavirus spike proteins: implications for virus assembly. *J Virol* **64**, 339–346.

Versteeg, G. A., Slobodskaya, O. & Spaan, W. J. (2006). Transcriptional profiling of acute cytopathic murine hepatitis virus infection in fibroblast-like cells. *J Gen Virol* **87**, 1961–1975.

Yokomori, K. & Lai, M. M. (1992). The receptor for mouse hepatitis virus in the resistant mouse strain SJL is functional: implications for the requirement of a second factor for viral infection. *J Virol* **66**, 6931–6938.

Zhao, L., Rose, K. M., Elliott, R., Van Rooijen, N. & Weiss, S. R. (2011). Cell-type-specific type I interferon antagonism influences organ tropism of murine coronavirus. *J Virol* **85**, 10058–10068.